A Multi-Wavelength Pump Upgrade for High-Resolution tr-ARPES via High Harmonic Generation

Sanya Gowda[1*], Tran Nguyen[2*], Haoyue Jiang[3],

[1] Department of Statistics, UC Berkeley; [2] Department of Materials Science & Engineering, UC Berkeley; [3] Applied Sciences & Technology Graduate Group, UC Berkeley.
* These authors contributed equally to this work.

1 MOTIVATION

Many essential processes in materials—such as charge transfer, phase transitions, and symmetry breaking—unfold on **ultrafast timescales**, often within femtoseconds. Capturing these dynamics requires not only fast measurement tools but also precise control over how the system is excited. Using pump pulses at **multiple wavelengths** allows us to selectively excite different energy states, offering greater flexibility in probing and steering material responses.

Key Upgrades:

- **Hardware**: Added a 515 nm pump laser using second harmonic generation (SHG)
- **Diagnostics**: Measured beam profile, intensity, and SHG conversion efficiency

2 BACKGROUND

Time-resolved Angle-Resolved Photoemission Spectroscopy (**tr-ARPES**) captures how a material's electronic structure evolves on femtosecond timescales, revealing ultrafast processes like phase transitions and carrier dynamics. Conventional 6-7 eV source limit access to the full Brillouin zone, restricting momentum resolution. Synchrotrons offer broader coverage but lack ultrafast resolution and in-lab flexibility.

By using High Harmonic Generation (**HHG**), we generate ~21.8 eV XUV pulses that access the full Brillouin zone beyond the Γ-point. This enables momentum-resolved studies of spin-orbit coupling, band splitting, and nonequilibrium many-body interactions. The ~210 fs pulses are isolated without a monochromator, and high repetition rates help suppress space-charge effects for improved energy resolution.

To enable flexible pump configurations, we convert 1030 nm pulses to 515 nm via second-harmonic generation in a Type I BBO crystal. Polarization control ensures phase matching for efficient SHG and clean beam separation. This modular design supports current multi-wavelength excitation and lays the foundation for future implementation of tunable pump wavelengths.

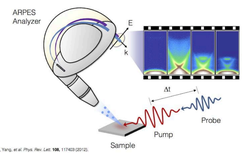

Fig. 1. ARPES experimental geometry with hemispherical energy analyzer

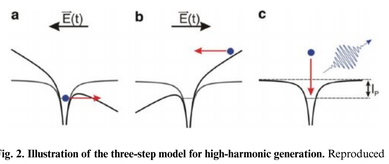

Fig. 2. Illustration of the three-step model for high-harmonic generation. Reproduced from Roling & Zacharias (2010), Coherence of XUV Laser Sources, ResearchGate. a) deformation of the atomic potential and tunnel ionization of the target atoms (b) acceleration of the free electrons in the laser electric field (c) recombination and photon emission

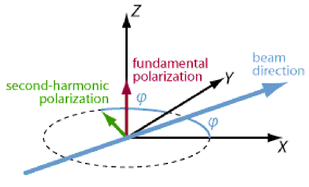

Fig. 3. Paschotta, Rüdiger, et al. Critical Phase Matching (2005)

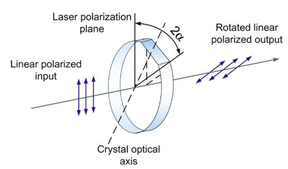

Fig. 4. Polarization of Light Through a Half Wave Plate

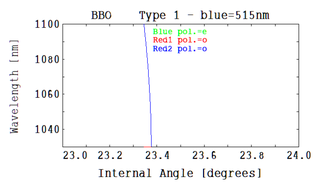

Fig. 5. SNLO graph depicting the necessary cut angle for BBO

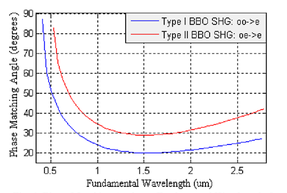

Fig. 6. Phase Matching Angles vs Fundamental Wavelength for Type I and Type II BBO Crystal SHG

3 EXPERIMENTAL SETUP

Key Optical Components Added:

- **BBO Crystal (β Barium Borate)**: Converts 1030 nm to 515 nm via nonlinear frequency doubling.
- **Half Waveplate**: Rotates polarization to match the crystal axis.
- **Polarizer**: Filters polarization for consistent harmonic output.

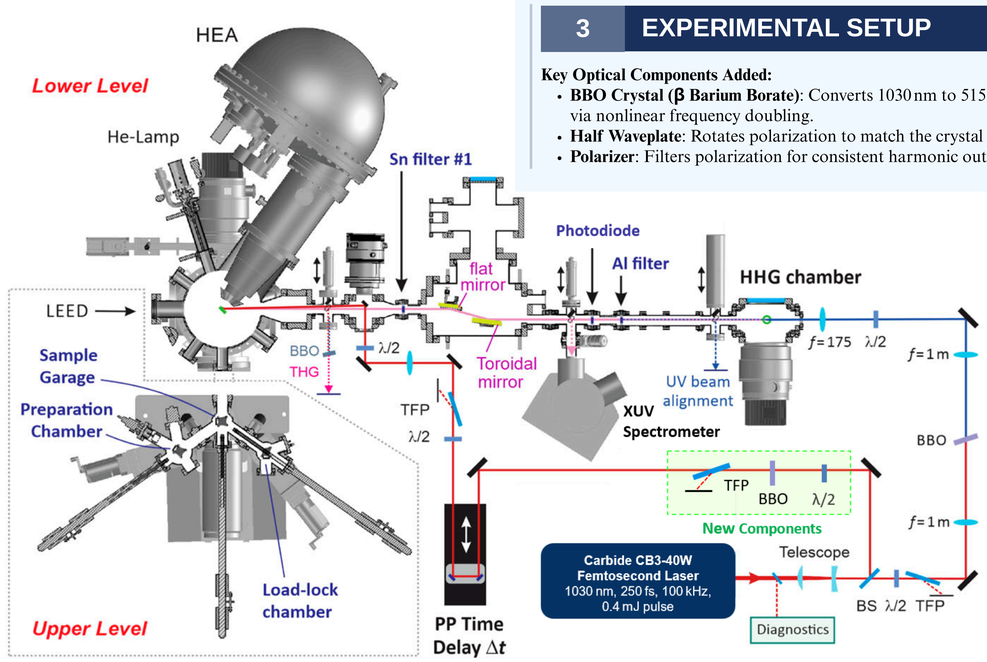

Fig. 7. Technical Overview of the laser setup. Adapted from Buss et al., Rev. Sci. Instrum. 90, 023105 (2019), with modifications.
TFP: thin film polarizer, λ/2: half-wave plate, BS: beam splitter, BBO: β-barium borate, THG: third-harmonic generation, HEA: hemispherical electron analyzer, LEED: low-energy electron diffraction.

4 PROCEDURE

Probe To enable second-harmonic generation (SHG), we integrated a half-wave plate, BBO crystal, and thin-film polarizer, selected for phase-matching compatibility, polarization control, and damage tolerance at 515 nm. The waveplate rotated the laser's polarization to align with the BBO's Type I phase-matching axis, while the polarizer filtered out unwanted non-S-polarized light.

The setup **(1) uses a BBO crystal cut at 23.4°**, the angle calculated using SNLO for 1030 nm to 515 nm conversion at 300 K (Fig. 5), and **(2) has a fine-tuned orientation** to maximize SHG output. The waveplate remained fixed to ensure consistent input polarization. (3) **The additional varied laser input power** showcased how SHG output scaled with intensity, based on peak output readings from a power meter.

(4) Beam quality was evaluated using the WinCamD-UCD12 profiler at three points: the camera was placed before the BBO, after the BBO, and along the pump beam path. Neutral density filters prevented sensor damage, and the DataRay software provided ellipticity, width, and Gaussian fit parameters for beam diagnostics (Fig. 8).

Pump To optimize HHG output, we (5) **gradually reduced Kr gas flow in the HHG chamber while monitoring signal strength** via a photodiode connected to an oscilloscope. Voltage changes indicated relative harmonic intensity, helping identify the flow rate that yielded maximum HHG efficiency.

	Ellipticity	Major Axis (μm)	Minor Axis (μm)	X-Axis Gaussian Fit (%)	Y-Axis Gaussian Fit (%)	Plateau Uniformity	ADC Peak (%)
Before BBO (a)	0.71	6356.2	4489.8	93.9	96.4	0.12	91.1
After BBO (b)	0.91	1556.8	1417.4	96.4	95.4	0.14	90.1
Pump (c)	0.80	4549.8	3622.3	93.2	91.0	0.14	86.8

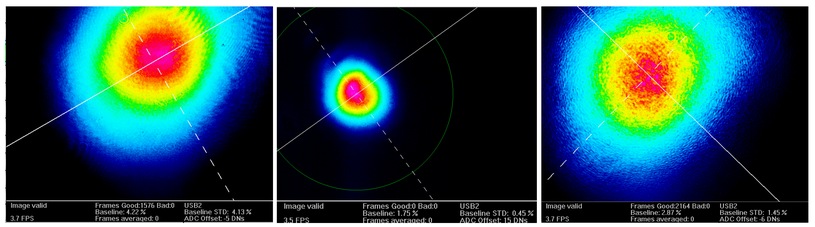

(a) (b) (c)

Fig. 8. Beam profiles measured at three key points in the optical path: (a) before BBO (fundamental), (b) after BBO (second harmonic), and (c) pump beam
Profiles illustrate beam shape evolution and spatial quality across conversion stages.

5 RESULTS

The **SHG efficiency** measurements across various rates reveal a clear dependence on pulse energy. At 50 kHz and 75 kHz, higher pulse energies enabled conversion efficiencies at lower input wattages, while 100 kHz and 200 kHz showed reduced performance due to lower per-pulse energy. These results highlight that lower repetition rates yielded higher SHG efficiency, underscoring the importance of optimizing pulse energy and alignment.

The **HHG signal**, measured via oscilloscope across a range of gas flow rates, demonstrated that higher harmonics are more efficiently generated at lower repetition rates. The 50 kHz configuration illustrated below in Fig. 9 produced significantly stronger signals than 100 kHz, consistent with the higher peak intensities available at lower frequencies. The polynomial fits further emphasize the saturation behavior of harmonic output with increasing flow, indicating an optimal operating window for gas pressure.

The observed **increase in efficiency** compared to previous setups can be attributed to improved beam alignment and the integration of new optical components, including a high-quality BBO crystal, polarization control elements, and a more stable 1030 nm laser source. These upgrades helped ensure consistent phase matching and polarization, both of which are critical for maximizing nonlinear conversion processes like SHG and HHG.

Fig. 9. Harmonic Intensity vs Flow rate with Fitting

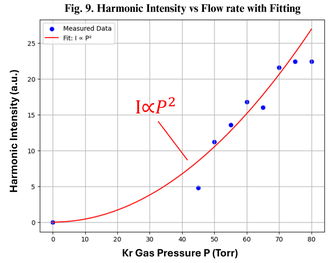

Fig. 10. SHG Efficiency vs Input Power Graph

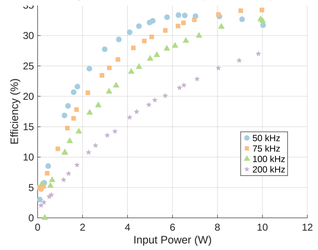

Fig. 11. Laser Entering Kr Gas Cell in the HHG Chamber

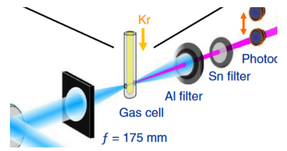

Fig. 12. SHG Efficiency vs Input Power Peak Efficiency Table

Repetition Rate	Efficiency (%)	Input Power (W)
50 kHz	33.36	6.265
75 kHz	34.182	9.976
100 kHz	32.674	9.916
200 kHz	46.277	0.188

Fig. 13. kx scan at Weyl point (Equilibrium)

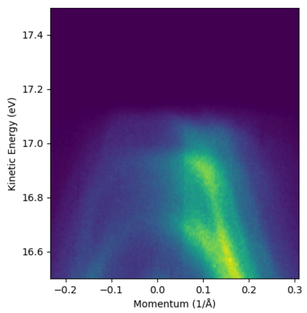

Fig. 14. kx scan at Weyl point (Excited)

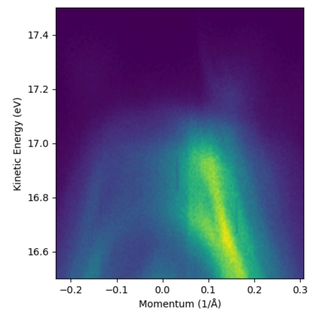

6 ACKNOWLEDGEMENTS

This research was supported by the Kavli Energy NanoScience Institute (ENSI), Berkeley Discovery, and Lawrence Berkeley National Laboratory. We thank the staff and mentors for their guidance and support throughout this project. We also thank Haoyue Jiang for her consistent support and mentorship throughout this project.

Fig. 7: Buss, J. H., Wang, H., Xu, Y., Maklar, J., Joucken, F., Zeng, L., ... & Kaindl, R. A. (2019). A setup for extreme-ultraviolet ultrafast angle-resolved photoelectron spectroscopy at 50-kHz repetition rate. Review of Scientific Instruments, 90(2), 023105. https://doi.org/10.1063/1.5079677

Fig. 5 & 6: Smith, A. V. (n.d.). SNLO nonlinear optics software [Computer software]. AS-Photonics. Smith, A. V. SNLO Nonlinear Optics Software, AS-Photonics, www.as-photonics.com